

Comparative simulation study of colloidal gels and glasses

Antonio M. Puertas*, Matthias Fuchs and Michael E. Cates

Department of Physics and Astronomy, The University of Edinburgh, EH9 3JZ, UK

(October 24, 2018)

Using computer simulations, we identify the mechanisms causing aggregation and structural arrest of colloidal suspensions interacting with a short-ranged attraction at moderate and high densities. Two different non-ergodicity transitions are observed. As the density is increased, a glass transition takes place, driven by excluded volume effects. In contrast, at moderate densities, gelation is approached as the strength of the attraction increases. At high density and interaction strength, both transitions merge, and a logarithmic decay in the correlation function is observed. All of these features are correctly predicted by mode coupling theory.

Colloidal dispersions aggregate into various non-equilibrium structures depending on density, interaction strength and range. The accompanying rheology and structure are among the key properties desired for their technological applications [1]. Moreover, thanks to the possibility to tailor effective interactions by e.g. addition of salt and polymer, colloids allow us to study the fundamental mechanisms of kinetic arrest. Whereas colloidal hard spheres have become a model system for the study of structural arrest at a glass transition [2], colloidal gelation has only recently been associated with glassy behavior [3–5]. Colloidal gelation is ubiquitous in suspensions driven by attractions of quite short range and moderate to high strength [6]. At low packing fractions, it entails the formation of heterogeneous and often self-similar networks; there, an interplay of phase separation kinetics and percolation often are considered responsible for its existence [6]. At higher densities, the gelation boundary extends into the homogeneous fluid region [3, 7], where it also lies well separated from estimates of percolation [3, 7–9]. Crossing into the gelled state anywhere along the transition line results in qualitatively the same phenomena, like flow properties that indicate solidification [7, 8], and non-ergodic dynamics according to light scattering [3, 10, 11].

We present simulations designed to identify the mechanism of colloidal gelation driven by attractions of only moderate strength. Because of the distance of the gel boundary from other boundaries (percolation and phase separation) at higher densities, we concentrate on these, where we sweep out the region between gel and glass transition lines. We show that both non-equilibrium transitions are caused by a slowing down of local rearrangements, as predicted well by mode coupling theory (MCT) [4, 12, 13]. We contrast the glass transition, caused by caging of particles owing to steric hindrance, with attraction-driven gelation caused by bonding between particles. We verify that the simultaneous presence of two non-ergodic states results in anomalous non-exponential (logarithmic) time dependences, as recently

conjectured to explain observations in micellar systems [9] or microgel suspensions [14].

The simulated system comprises 1000 soft-core ($V(r = |\mathbf{r}_i - \mathbf{r}_j|) \propto (a_{ij}/r)^{36}$, $a_{ij} = a_i + a_j$) particles of mean radius a with polydispersity in size (flat distribution with 10% width) to prevent crystallisation. Densities are reported as packing fractions $\phi_c = \frac{4\pi}{3}na^3$. A short range attraction, mimicking the polymer induced depletion attraction in experimental systems [1, 6, 10, 11], is given by an Asakura-Oosawa (AO) form generalized to polydisperse systems [15, 16]. The range of the attraction, 2ξ , is set to $0.2a$, and its strength is proportional to the polymer concentration ϕ_p . To help avoid liquid-gas separation, a weak long range barrier is added to the potential. The barrier extends from $a_{12} + 2\xi$ to $4a$, and is described by a fourth order polynomial matched to give a continuous force. Its maximal height is $1k_B T$, which equals the depth at contact of the AO potential at $\phi_p = 0.0625$. In all states studied, the barrier is much smaller than the attraction, and in the purely repulsive case ($\phi_p = 0$) it is omitted. We will measure lengths in units of a and time in units of $\sqrt{4a^2/3v^2}$, where the thermal velocity, v , is set to $2/\sqrt{3}$. Equations of motion were integrated using the velocity-Verlet algorithm, with a time step of 0.0025. Colloidal dynamics (neglecting hydrodynamic interactions) were mimicked by running the simulations in the canonical (constant NTV) ensemble, where the thermostat plays the role of the surrounding liquid. Every N time steps, the velocity of the particles was rescaled to assure constant v . No effect of N on the results was observed for well equilibrated samples.

The central quantity of our study will be the self part of the intermediate scattering function, $\Phi_q^s(t) = \langle \exp i\mathbf{q} \cdot (\mathbf{r}_j(t) - \mathbf{r}_j(0)) \rangle$, for wave-vector \mathbf{q} , where $\langle \dots \rangle$ denotes an average over particles and time origin. $\Phi_q^s(t)$ allows us to probe and identify the nature of the dominant dynamical mechanism because of (i) its q -dependence and (ii) the detailed predictions that are available from MCT. Indeed, if a structural arrest at a non-ergodicity transition is approached, $\Phi_q^s(t)$ reveals a two-step pro-

cess, where the decay from the plateau is given by the von Schweidler power-law series [17]:

$$\Phi_q^s(t) = f_q^s - h_q^{(1)}(t/\tau)^b + h_q^{(2)}(t/\tau)^{2b} + O(t^{3b}). \quad (1)$$

Here f_q^s is the non-ergodicity parameter, $h_q^{(1)}$ and $h_q^{(2)}$ are amplitudes, and b is known as the von Schweidler exponent. On the one hand, the observation of this (universal) von Schweidler behavior – and tests of further relations, as done below – establishes that a feed-back mechanism in the structural relaxation causes arrest. On the other hand, the (non-universal) wave-vector dependence of the amplitudes, like f_q^s , allows us to identify the specific kinetic process which freezes out. As the transition is approached, the characteristic time τ diverges as $\tau \propto |\phi - \phi^c|^{-\gamma}$, where γ is determined by b , see e.g. [17].

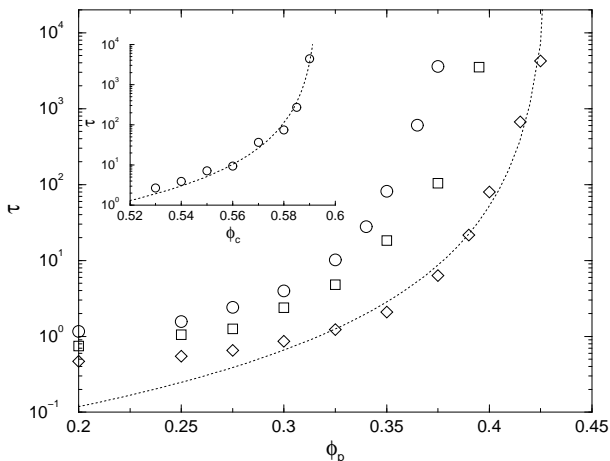


FIG. 1. Relaxation time τ as a function of ϕ_p for three colloid volume fractions: $\phi_c = 0.40$ (\diamond), $\phi_c = 0.50$ (\square), $\phi_c = 0.55$ (\circ). Inset: τ vs. ϕ_c for soft spheres ($\phi_p = 0$, $V(r) \sim r^{-36}$). Dotted lines are fittings with predetermined γ .

Figure 1 presents evidence for both the repulsion and attraction driven glass transitions, as identified by a diverging τ [18]. Upon increasing the packing fraction ϕ_c (inset in figure 1), the system approaches a glass transition caused by steric hindrance, which we have studied including only the r^{-36} repulsion ($\phi_p = 0$ and no barrier) [19]. The transition correlates well with observations at the colloidal glass transition [2] and previous simulations of e. g. a glassy Lennard-Jones mixture [20]. We have analysed it using the concepts of idealized MCT, but will present only a few results here for comparison with gelation. Gelation itself is induced by strengthening the attraction at intermediate packing fractions (figure 1). There, far from equilibrium or percolation transitions (as we tested by monitoring the static structure factor), arrest again is of kinetic origin, and occurs at lower attraction strengths the higher ϕ_c .

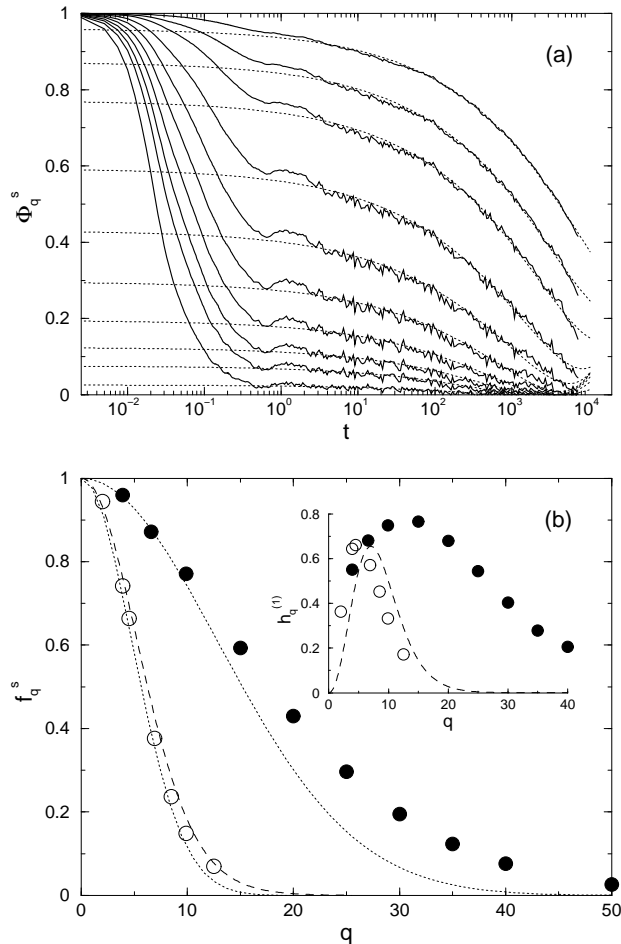


FIG. 2. (a): Correlation functions at $\phi_c = 0.4$, $\phi_p = 0.425$ and von Schweidler fits. From top to bottom, $q = 3.9, 6.9, 9.9, 15, 20, 25, 30, 35, 40, 50$. (b): f_q^s for glass (\circ) and gel (\bullet) (from (a)) transitions, with the Gaussian approximation for both of them (dotted lines) and the MCT result for hard spheres (dashed line) [22]. Inset: $h_q^{(1)}$ using τ from figure 1, and MCT result for hard spheres.

To shed light on this transition, the correlation functions at different wave-vectors were studied. The slowest state at $\phi_c = 0.40$ is presented in Fig 2. The upper panel shows the self intermediate scattering functions for different wave-vectors, and the fits using (1) up to second order. A common exponent b was taken in the fitting, yielding a value of $b = 0.38$, appreciably lower than the hard spheres value $b = 0.53$ (which we found for our soft sphere glass at $\phi_p = 0$). As predicted by MCT, we can calculate from b the divergence of the relaxation times in Fig. 1. The resulting value $\gamma = 3.03$ fits the data, while $\gamma = 2.63$ at the soft sphere glass transition [19]. The gel transition is estimated to occur at $\phi_p = 0.431$. Because we find the universal properties predicted by MCT, we conclude that at $\phi_c = 0.40$ the gel transition is a regular non-ergodicity transition in the structural dynamics.

Their very different q -width (Fig. 2b) for the non-ergodicity parameters and amplitudes brings out a major

difference in the two underlying mechanisms. Whereas repulsions localize the particle within a cage, which it can explore up to mean squared displacements r_l^2 of the order of $r_l^2 = 0.13$ (from our simulations, not shown; $r_l^2 = 0.134$ from MCT [22]), attractions bind the particle to its neighbors and thus localize it much more tightly. At $\phi_c = 0.40$, we find $r_l^2 = 0.018$ by simulations, which is of the order of a low-density estimate [4] for our interaction range, $2\xi = 0.2$. The corresponding high amplitudes f_q^s of density fluctuations are consistent with light scattering observations at fixed q [10, 11] and with MCT calculations [4, 12, 13]. These fluctuations extend to large q and relax only when the particles break free from their bonds. The comparison with the Gaussian approximation, $f_q^{sG} = \exp\{-q^2 r_l^2/6\}$ evidences stronger non-Gaussian effects at gelation than at the glass transition. We stress the cooperativity of the structural relaxation at both transitions. Holding all particles fixed, except for one, leads to mean squared displacement for the tracer (as it explores the frozen environment) much smaller than in the free system (before the start of the structure relaxation of the free system, the ratio is ≈ 6 for both cases). The cage or network of bonds around an arrested particle thus necessarily fluctuates with it.

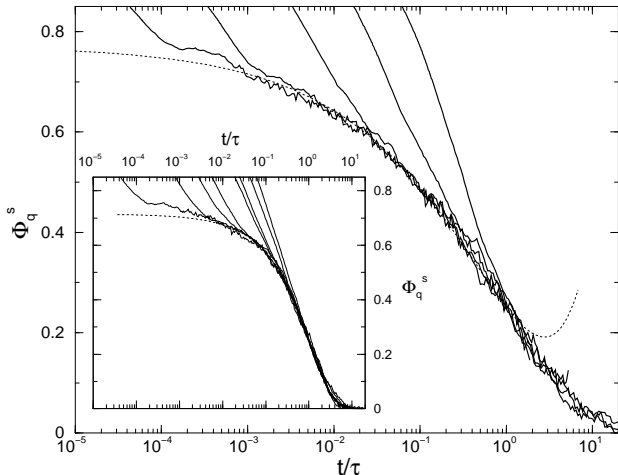


FIG. 3. Correlation functions vs. rescaled time t/τ for $\phi_c = 0.4$ and $\phi_p = 0.375, 0.39, 0.40, 0.415, 0.425$ (from right to left) and von Schweidler fit. Inset: Same plot for soft spheres and $\phi_c = 0.53, 0.54, 0.55, 0.56, 0.57, 0.58, 0.585, 0.59$, and MCT master curve [22].

To test further the nature of the gel transition, the scaling of the final (or α -) decay was studied. In Fig. 3 we present the rescaled ($\Phi_q^s(t/\tau = 1) = 0.25$) correlation functions at $q = 9.9$ for different attraction strengths, close to the gel transition. In the inset to this figure, a similar plot deals with the glass transition ($q = 3.9$ in this case). In both cases, the curves clearly collapse during the α -decay indicating an unique mechanism which dominates the slowing down at the transitions. For the purely repulsive case, the MCT master curve for the rescaled de-

cay of hard spheres [22] at a slightly larger wave-vector ($q = 4.3$) is also presented, confirming the quantitative agreement between MCT and our results. In the gel case, no master function is available, but the fit to (1) is presented. The different stretching in the two cases is clear.

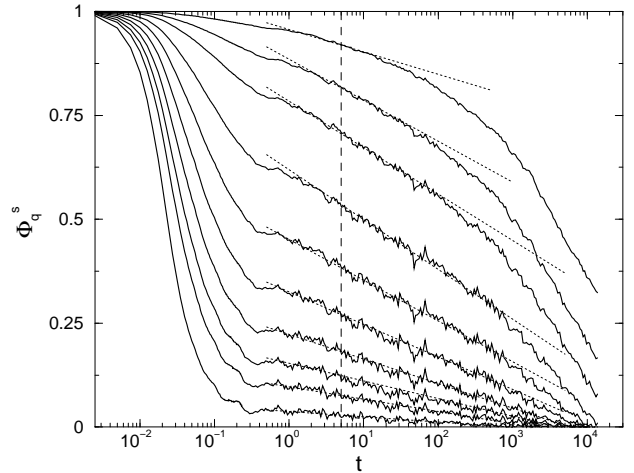


FIG. 4. Same as figure 2(a) for $\phi_c = 0.55$ and $\phi_p = 0.375$. Dotted lines: logarithmic fittings to the correlators around f_q^s . The dashed line represents t_1 .

We study now the gel transition at a higher density $\phi_c = 0.55$, where it lies closer to the glass transition. Within MCT, the simultaneous existence of two different non-ergodicity transition branches opens the possibility for end-point singularities, where the branches merge [21]. In systems with short range attractions, such a singularity has been predicted close to the crossing of the two transition lines (the actual distance depending on the details of the potential) [4, 12, 13]. Close to the singularity, a logarithmic decay around the plateau in the correlation function, $\Phi_q^s(t) = f_q^{sA} - C_q \ln(t/t_1)$, is a proposed signature [12, 13], and intriguingly is observed experimentally in more complicated systems [9, 14]. Having identified two different non-ergodicity transitions in our system, we now test this prediction. In Fig. 4, the correlation functions at the same wave-vectors as in Fig. 2 are presented for the state $\phi_p = 0.375$. Logarithmic decays are observed in all of the correlators (linear traces in the plot) for up to three decades in time, signalling a higher order singularity nearby. It is interesting to note that the logarithmic trace of the correlator has different extents, depending on the wave-vector. To make it clearer, $(\Phi_q^s - f_q^{sA})/C_q$ vs. time has been plotted as an inset to Fig. 5, where f_q^{sA} is determined at $t_1 = 5$ (vertical line in Fig. 4). Deviations from the logarithmic decay are stronger, the higher f_q^s . This is in complete agreement with the theoretical expectations in [13]. Since both the von Schweidler decay (associated with the gel transition) and the logarithmic trace now take place in the same window, important corrections to the α -scaling of the

curves are expected. This is seen in the main graph of Fig. 5: the long time dynamics at different states cannot be collapsed onto a master curve by time rescaling. This shows that two mechanisms are responsible for the structural slowing down and that changes in the control parameters change the relative distance to gelation but also to the higher order singularity. The intermediate isochore, $\phi_c = 0.50$, shows a mixed behavior: a logarithmic decay in a smaller window than for $\phi_c = 0.55$, and followed by an apparent power law decay.

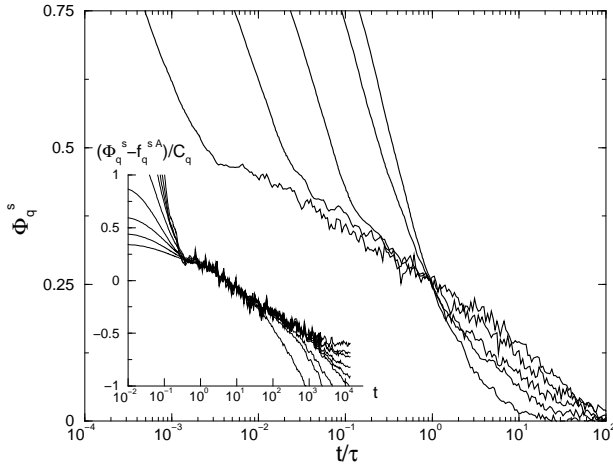


FIG. 5. Correlation function vs. rescaled time, t/τ , at $q = 20$. $\phi_c = 0.55$, and $\phi_p = 0.325, 0.34, 0.35, 0.365, 0.375$ from right to left at $t < \tau$. Inset: $(\Phi_q^s - f_q^{sA})/C_q$ as a function of time for the same state and wave-vectors as figure 4 (wave-vectors increasing from top to bottom).

In summary, using MD simulations, we have deduced from the wave-vector dependence of the dynamical density fluctuations, that repulsion and short-ranged attraction lead to two different structural arrests at high enough density or attraction strength, respectively. At the merging of both glassy states, subtle logarithmic time variations appear. Comparing with the recent MCT predictions of these phenomena we find perfect agreement.

We thank W. Kob for valuable discussions. M.F. was supported by the Deutsche Forschungsgemeinschaft, grant Fu 309/3, and A.M.P. by the Ministerio de Educación y Cultura.

* Permanent address: Department of Applied Physics, University of Almería, 04.120 Almería, Spain.

- [1] W. B. Russel, D. A. Saville, and W. R. Schowalter, *Colloidal Dispersions* (Cambridge University Press, New York, 1989).
- [2] W. van Meegen, T.C. Mortensen, S.R. Williams and J. Müller, *Phys. Rev. E* **58**, 6073 (1998); and references therein.
- [3] H. Verduin and J. K. G. Dhont, *J. Colloid Interface Sci.* **172**, 425 (1995).
- [4] J. Bergenholtz and M. Fuchs, *Phys. Rev. E* **59**, 5706 (1999).
- [5] P. N. Segrè, V. Prasad, A. B. Schofield and D. A. Weitz, *Phys. Rev. Lett.* **86**, 6042 (2001).
- [6] W. C. K. Poon and M. D. Haw, *Adv. Colloid Interface Sci.* **73**, 71 (1997); and references therein.
- [7] M. C. Grant and W. B. Russel, *Phys. Rev. E* **47**, 2606 (1993).
- [8] C. J. Rueb and C. F. Zukoski, *J. Rheology* **42**, 1451 (1998).
- [9] F. Mallamace *et al.*, *Phys. Rev. Lett.* **84**, 5431 (2000).
- [10] W. C. K. Poon *et al.*, *Faraday Discuss.* **112**, 143 (1999).
- [11] K. Pham *et al.*, in preparation (2001).
- [12] L. Fabbian *et al.*, *Phys. Rev. E* **59**, R1347 (1999); **60**, 2430 (1999).
- [13] K. Dawson *et al.*, *Phys. Rev. E* **63**, 011401 (2001).
- [14] E. Bartsch, V. Frenz, and H. Sillescu, *J. Non-Cryst. Solids* **172-174**, 88 (1994). Private communication.
- [15] J.M. Méndez-Alcaraz and R. Klein, *Phys. Rev. E* **61**, 4095 (2000).
- [16] The potential minimum was set to a_{12} using a parabola for $r < a_{12} + \xi/5$, smoothly connected to the AO.
- [17] T. Franosch *et al.*, *Phys. Rev. E* **55**, 7153 (1997); M. Fuchs, W. Götze, and M. R. Mayr, *Phys. Rev. E* **58**, 3384 (1998); and references therein.
- [18] The relaxation time was defined by $\Phi_q^s(t = \tau) = 0.25$ at $q = 3.9$ for the glass transition and $q = 9.9$ for gelation.
- [19] The glass transition was shifted from $\phi_c = 0.594$ to $\phi_c = 0.55$, upon inclusion of the barrier. No qualitative differences were observed.
- [20] W. Kob, in *Soft and Fragile Matter*, edited by M.E. Cates and M.R. Evans (Institute of Physics Publishing, Bristol, 2000), p. 259.
- [21] W. Götze and L. Sjögren, *J. Phys. Condens. Matter* **1**, 4203 (1989).
- [22] J. L. Barrat, W. Götze and A. Latz, *J. Phys. Condens. Matter* **1**, 7163 (1989); M. Fuchs, I. Hofacker and A. Latz, *Phys. Rev. A* **45**, 898 (1992).